Available online at www.sciencedirect.com
ScienceDirect
Solid State Communications 145 (2008) 407–412
solid state communications
www.elsevier.com/locate/ssc

Structural phase transition in ferroelectric glycine silver nitrate

Rajul Ranjan Choudhury[a,*], Lata Panicker[a], R. Chitra[a], T. Sakuntala[b]

[a] *Solid State Physics Division, Bhabha Atomic Research Center, Trombay, Mumbai 400085, India*
[b] *High Pressure Physics Division, Bhabha Atomic Research Center, Trombay, Mumbai 400085, India*

Received 25 June 2007; received in revised form 25 October 2007; accepted 10 November 2007 by D.D. Sarma
Available online 19 November 2007

Abstract

The structural investigation of the ferroelectric phase transition in glycine silver nitrate has revealed that the transition at $T_c = 218$ K is due to the displacement of the Ag^+ ions from the plane made by the carboxyl oxygens of glycine zwitterions coordinated to it. Since the transition takes place between two ordered structures the thermal anomaly at T_c is very weak, the transition enthalpy and transition entropy were found to be $\Delta H = 6.6$ J/mol and the transition entropy $\Delta S = 0.03$ J K^{-1} mol^{-1} respectively. These crystals are held together by a network of hydrogen bonds. In order to study these interactions the Raman spectrum of GSN was recorded and discussed in the light of ferroelectricity in glycine complexes in general.

PACS: 77.80.-e; 77.80.Bh; 61.10.Nz

Keywords: A. Ferroelectrics; C. X-ray scattering; D. Phase transitions; D. Heat capacity

1. Introduction

Ferroelectricity has been discovered in many of the glycine complexes like triglycine sulfate (TGS) [1], triglycine selenate (TGSe) [1], triglycine fluroberylate (TGFBe) [1], diglycine nitrate (DGN) [2], glycine silver nitrate (GSN) [3], glycine phosphite (GPI) [4] etc. The glycine molecule is a non-rigid molecule having three internal rotational degrees of freedom which result in a large number of rotational conformers of which the lowest energy conformer is planar [5] i.e. it is achiral. The non-planar conformers have small interconversion barriers to the lowest energy planar conformer. As a result the conformation of the glycine molecule can be easily altered by the cooperative effects [6] like the long-range dipolar interaction within the crystalline environment. This can be one of the reasons for a number of glycine complexes to undergo symmetry breaking structural phase transitions.

All the above mentioned glycine complexes are hydrogen-bonded crystals and the ferroelectric phase transition in all of these complexes with the exception of glycine silver nitrate is found to be of order–disorder type. This fact makes the study of the structural phase transition in GSN interesting and important in order to understand ferroelectricity in glycine complexes. The crystal symmetry of GSN is lowered from $P2_1/a$ to $P2_1$ at the transition point $T_c = 218$ K [3]. Rao and Viswamitra [7] had determined the ambient temperature crystal structure for GSN in 1972 but no ferroelectric phase structure has been reported to the present; this is due to the fact that GSN crystals are light sensitive and hence the single crystal diffraction data needs to be collected fast. Though the infrared study [8] and the proton magnetic resonance study [9] on GSN have indicated that ferroelectricity in GSN is in all probability due to the motion of the silver ions (Ag^+). Since silver is a very good scatterer of X-rays the above stated change at the transition point can be very effectively studied by X-ray powder diffraction. In the present work an X-ray powder diffraction study on GSN was undertaken to elucidate the low temperature structure and investigate the origin of ferroelectricity in these crystals.

Since the ferroelectric phase transition in GSN is in all probability displacive type the thermal anomaly at the transition temperature is expected to be weak; this fact has been theoretically indicated by the coupled anharmonic oscillator model for ferroelectrics [10]. Very weak thermal anomaly at

* Corresponding author.
E-mail address: rajulranjan@gmail.com (R.R. Choudhury).

0038-1098/$ - see front matter © 2007 Elsevier Ltd. All rights reserved.
doi:10.1016/j.ssc.2007.11.010

T_c in GSN was recorded using a high resolution differential scanning calorimeter. A comparison with the other ferroelectric glycine complexes is reported.

Hydrogen bonding plays a very important role in determining the physical properties of these soft molecular solids. Understanding the effect of hydrogen bonding on the ferroelectric behavior of the glycine complexes can throw light on the properties of hydrogen-bonded ferroelectrics in general. In order to study the hydrogen bonding in GSN a Raman spectrum was recorded at room temperature and discussed in the light of ferroelectricity in glycine complexes in general. This to the best of our knowledge is the first ever Raman study on GSN.

2. Experiment

Crystals of GSN were grown in the dark by slow evaporation of an aqueous solution of glycine and silver nitrate mixed together in 1:1 stoichiometric ratio. It was observed that the crystals became brown after prolonged exposure to intense light like direct sunlight.

DSC measurement on these crystals of GSN in the temperature range 173–473 K with heating rate of 10 K/min was performed using a differential scanning calorimeter (Metler Toledeo make) in order to measure the change in the specific heat at the transition point.

GSN crystals were powdered and loaded on an X-ray sample holder in the dark; this was then loaded on a Rigaku *R*-axis D-max powder diffractometer coupled to a rotating anode generator (Rigaku make). The sample chamber was covered from the top so as to minimize the light exposure to the sample. The room temperature X-ray pattern was recorded at 6 KW X-ray power using Cu Kα wavelength for the 2θ range 15°–70° at a step of 0.02° with 2.3 s of recording time per step. The complete pattern was recorded within 1.8 h (Fig. 1(a)); since the pattern had to be recorded fast no further improvement of data statistics especially in the high angle regions could be obtained. This fact is reflected in the higher Rexp values in the Rietveld refinement. At this stage no change in the colour of the sample was observe indicating that the sample had not started decomposing. Cold nitrogen gas jet at 168 K from an Oxford cryojet was used to cool the sample below the transition point (218 K). The X-ray pattern was once again recorded under the same conditions as described above (Fig. 1(b)). Some frosting around the sample holder was observed while recording the low temperature diffraction pattern and so a blank run for the empty sample holder was recorded (Fig. 1(c)) in the end under identical conditions as described above. The regions where there could be a possibility of some extra peaks due to the ice crystals were excluded from the low temperature data during the structure refinement.

The Raman spectrum of GSN crystal was recorded using the 532 nm laser line. Power on the sample was kept below 10 mW to reduce the radiation damage. Crystals were found to be stable and not decomposing during the experimental time. Scattered light was detected using a CCD-based (Andor Technology) spectrograph consisting of a home-built 0.9 m monochromator

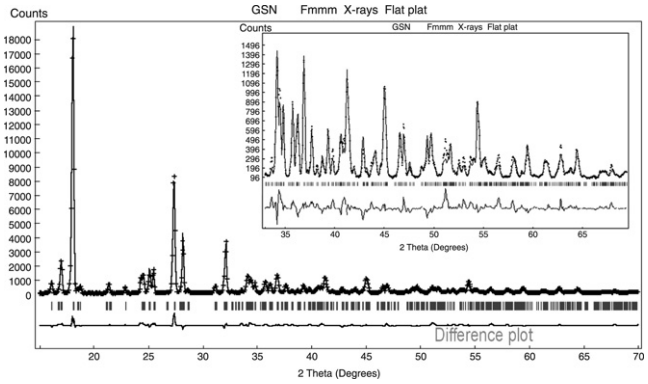

(a) Room temperature.

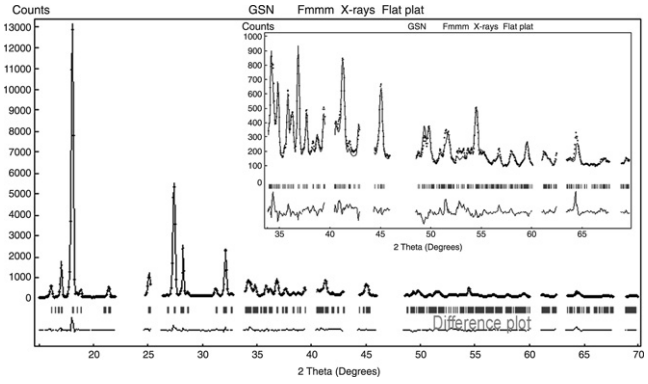

(b) Low temperature.

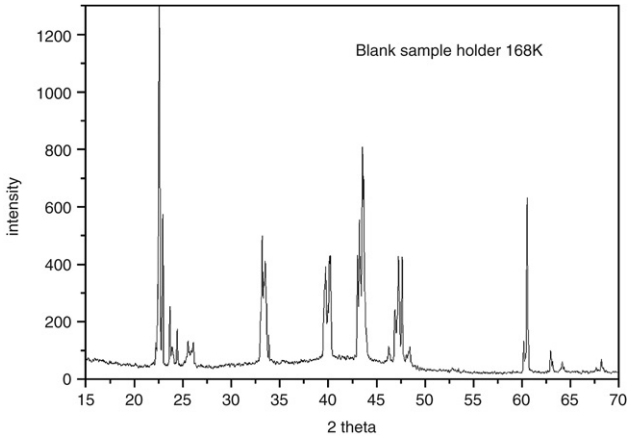

(c) Blank sample holder at ∼168 K.

Fig. 1. Fit of the observed X-ray pattern of GSN to the calculated one: (a) at RT, (b) at ∼168 K. The figure in the inset is the magnified intensity scale for high-angle range, (c) blank sample holder at ∼168 K.

together with a super notch filter. Entrance slit was kept at 50 μm, which gives a spectral band pass of 3 cm^{-1}. The integration time for the recorded spectra was 50 s. The typical exposure time for recording a spectrum was 100 s.

3. Structure analysis

Rietveld structure refinement was carried out using X-ray diffraction data. The starting model was taken from the room temperature structure reported by Rao and Viswamitra [7]. In

Table 1
Rietveld refinement details

	Room temperature	Low temperature
2θ range	15°–70°	15°–70°
Peak shape	Split Pearson	Split Pearson
Space group	$P2_1/a$	$P2_1$
Cell parameters	$a = 5.443(1)$ Å, $b = 19.444(1)$ Å, $c = 5.537(1)$ Å, $\beta = 99.91(2)°$	$a = 5.424(2)$ Å, $b = 19.440(1)$ Å, $c = 5.544(2)$ Å, $\beta = 99.94(3)°$
Cell volume	577.3(3) Å^3	575.8(6) Å^3
Rietveld program	WinMProf [12]	WinMProf [12]
No. of parameter refined	23	31
Rp	11.11	10.82
Rwp	13.88	13.20
Rexp	6.88	8.14
Goof = Rwp/Rexp	2.01	1.621
$\chi 2$	4.07	2.63
RI	11.08	9.98

Table 2
Refined atomic coordinates of GSN at RT and LT (∼168 K)

Atom	x/a (LT)	y/b (LT)	z/c(LT)	x/a(RT)	y/b(RT)	z/c(RT)
Ag	0.396	0.004	−0.187	0.145	0.015	−0.177
N1	0.816	0.148	0.405	0.672	0.156	0.407
O2	0.539	0.054	0.128	0.395	0.062	0.130
C2	0.643	0.106	0.526	0.499	0.114	0.528
C1	0.482	0.060	0.335	0.338	0.068	0.337
O1	0.293	0.032	0.403	0.149	0.040	0.405
N2	0.271	0.171	−0.078	0.039	0.184	−0.047
O4	0.327	0.195	−0.270	0.095	0.208	−0.239
O3	0.375	0.190	0.131	0.143	0.203	0.162
O5	0.129	0.119	−0.086	−0.102	0.132	−0.055
Ags	0.107	−0.027	0.172			
N1s	−0.485	−0.159	−0.381			
O2s	−0.208	−0.064	−0.104			
C2s	−0.312	−0.116	−0.502			
C1s	−0.151	−0.071	−0.311			
O1s	0.037	−0.043	−0.379			
N2s	0.188	−0.198	−0.034			
O4s	0.132	−0.222	0.157			
O3s	0.084	−0.217	−0.244			
O5s	0.330	−0.145	−0.026			

The standard deviations in all the three coordinates are of the order of 0.001 at RT and 0.003 at LT.

order to reduce the number of parameters to be refined a rigid body refinement was done [11] where the conformations of the glycine zwitterion and the nitrate ion were fixed to that obtained from the single crystal X-ray diffraction study at RT. This is a reasonable approximation considering that no striking change in the infrared adsorption spectrum of GSN [8] in the internal mode region was observed when the temperature was lowered below T_c, indicating no drastic structural changes within the molecular ions. These ions as a whole were allowed to move within the unit cell; the refinement details are given in Table 1. Fig. 1(a) and (b) give the fit of the calculated pattern to the observed data along with the difference profile plot, which is the most important indicator of the Rietveld refinement [11]. Table 2 gives the atomic coordinates in the two phases; the origin is shifted by 0.25 along the a-axis in the low temperature phase.

4. DSC analysis

We have measured the weak thermal anomaly at the ferro-para phase transition in GSN (Fig. 2(a)), which could not be observed by the previous workers [3] due to their experimental limitations. The transition enthalpy was found to be $\Delta H = 6.6\,\mathrm{J\,mol^{-1}}$ and the transition entropy $\Delta S = 0.03\,\mathrm{J\,K^{-1}\,mol^{-1}}$.

In order to indicate that the phase transition in GSN is different from the order–disorder ferroelectric phase transition observed in other very well studied ferroelectric glycine complexes DSC measurements on TGS, TGSe and DGN crystals grown at our lab were conducted. Fig. 2 gives a comparison between the magnitudes of the thermal anomaly at T_c for all the four-glycine complexes. The fact that ΔH is hardly noticeable in GSN whereas it is easily measured in TGS [13], TGSe and DGN [14] indicates that the nature of the phase transition in GSN is different from the rest of

Table 3
Comparison between the melting temperature and melting enthalpy of some of the important ferroelectric glycine complexes

S. no.	Crystal	Melting temperature (K)	Ferroelectric transition temperature (K)	Melting enthalpy (kJ mol^{-1})
1	GSN	415	218	30.1
2	TGS	501	322	131.1
3	TGSe	471	295	Oxidation + 9.6 +decomposition
4	DGN	379	206	15.7
5	α-glycine	534	–	75.4

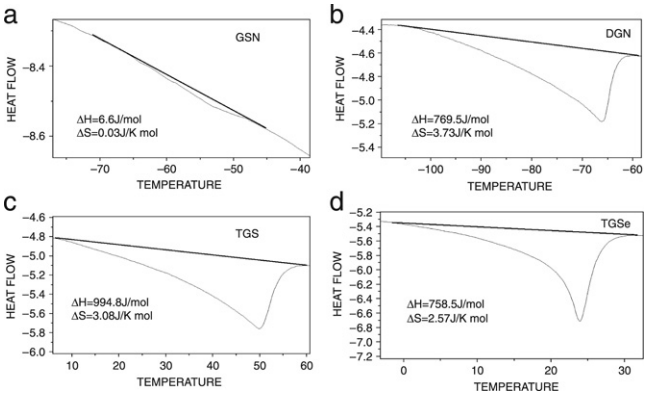

Fig. 2. Comparison of the anomaly in the specific heat at T_c for some of the important ferroelectric glycine complexes.

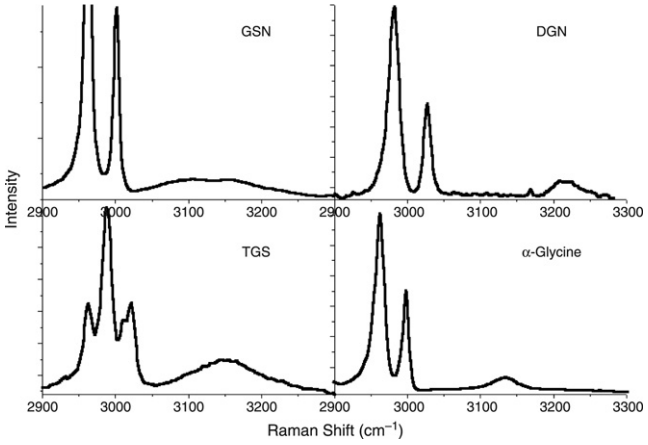

Fig. 3. Comparison between the Raman spectra in the NH–stretch region for alpha-glycine, GSN, DGN and TGS.

the complexes. In the displacive case transition takes place between two ordered structures; hence the transition entropy and enthalpy are small [15] as in the case of GSN, whereas in the order–disorder case, since the transition takes place from an ordered low temperature phase to a disordered high temperature phase, the transition entropy is of the order of R ln 2 as observed in TGS, TGSe and DGN.

Table 3 Comparison between the melting temperature and melting enthalpy of some of the important ferroelectric glycine complexes.

Table 3 gives a comparison between the melting point and melting enthalpy of GSN along with some of the other ferroelectric glycine complexes and pure glycine crystals. Melting point is a good indicative of the strength of hydrogen bonding in these molecular solids. An interesting point to be

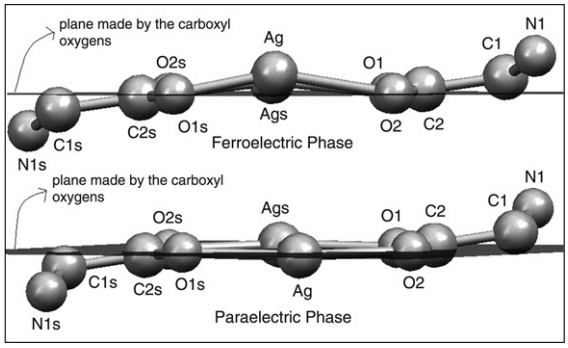

Fig. 4. Displacement of Ag^+ ions from the plane made by the carboxyl oxygens of glycine zwitterions in GSN.

noted from Table 3 is that transition temperature varies in the same order as the melting point in these glycine complexes.

5. Raman analysis

Crystals of alpha-glycine and all the above stated ferroelectric glycine complexes are held together by a three dimensional network of N–H–O type hydrogen bonds where the ionized amino group of glycine ions acts as a hydrogen bond donor, while the acceptor can be a oxygen atom of (a) carboxyl group of the glycine ion (alpha-glycine), (b) sulfate ion (TGS), (c) selenate ion (TGSe), (d) nitrate ion (DGN & GSN), or (e) phosphite ion (GPI). The strength of these hydrogen bonds can be studied by comparing the Raman spectra of these crystals in the internal mode region. The extent of red shift in N–H stretching frequency as well as blue shift in the frequencies of the bending vibrations is usually considered for understanding the relative strength of hydrogen bonding. A Raman spectrum of GSN was recorded at RT along with that of alpha-glycine under identical conditions in order to study the differences between the two. Since in a molecular crystal the intramolecular potentials are generally only weakly perturbed by the intermolecular interactions the internal vibrations of a molecule under different crystalline environments are similar. As a result one can make a comparison between the internal modes of a molecule like glycine in different crystalline environments. Hence the mode assignment (Table 4) was done by comparing the Raman frequencies of GSN in the internal mode region to those observed in the parent compounds alpha-glycine [16] and $AgNO_3$ [17]. The Ag–O stretch frequency is assigned based on the relation between Ag–O distance and the Ag–O stretch frequency as indicated by Gajdos et al. [18].

Fig. 3 shows the $-NH_3$ stretch region of glycine and some of the important ferroelectric glycine complexes. The most

Table 4
Assignment of internal Raman active modes of GSN and their comparison with modes of alpha-glycine and other ferroelectric glycine complexes

S. no.	GSN (cm^{-1})	Glycine[a] (cm^{-1})	TGS[b] (cm^{-1})	DGN[c] (cm^{-1})	$AgNO_3$[d] (cm^{-1})	Assignment
1	109	111				C–C tor
2	151	165				
3		181				
4	195	198				
5	210					Ag–O
6	358	358	330	338		CCN bend
7		493				CO_2 rock
8		503	498			CO_2 rock
9	599	602	578	583		CO_2 wag
10	692	697	673	684		CO_2 bend
11	706			707	709	ν_4NO_3
12	722			734	734	ν_4NO_3
13	825				809	ν_2NO_3
14	898	892	900	903		C–C str
15	908	922				CH_2 rock
16	1051			1058	1047	ν_1NO_3
17	1031	1034	1035			C–N str
18	1093	1108	1104			NH_3 rock
19	1107	1139	1114	1124		NH_3 rock
20	1305				1306	ν_3NO_3
21	1354			1340	1350	ν_3NO_3
22		1316	1301	1302		CH_2 twist
23	1330	1325	1323	1323		CH_2 wag
24	1415	1412	1414	1412		CO_2 sym str
25		1440	1441	1432		CH_2 bend
26	1451	1455	1480	1480		CH_2 sciss
27	1508	1504		1493		NH_3 def
28		1516		1523		NH_3 def
29	1556	1569	1538	1535		NH_3 def
30	1600			1595		NH_3 as bend
31	1630	1634				C–C str +CH2 wag
32		1670	1677	1657		CO_2 sym str
33	2858					
34	2891					
35	2973	2972	2988	2982		CH_2 sym str
36	3011	3008	3022	3029		CH_2 asym str
37	3093	3050				NH_3 sym str
38	3165	3144	3150	3208		NH_3 asym str

[a] J. Raman Spectrosc. 5 (1976) 49–55.
[b] J. Phys. Chem. Solids 55 (1994) 405–411.
[c] Spectrochim. Acta 51A (1995) 197–214.
[d] Raman Spectrosc. 23 (1992) 509–514.

important conclusion that one arrives at by comparing the –NH_3 stretch frequencies of the glycine complexes is that the strength of the N–H–O bond varies as follows: alpha-glycine > TGS > GSN > DGN. This fact is supported by observed variation in the melting points of these crystals (Table 3). The room temperature crystal structures of all ferroelectric glycine complexes were extracted from the Cambridge crystallographic database [19]. One observes N–O distances ranging from: (a) 2.770–2.955 Å in alpha-glycine, (b) 2.769–3.019 Å in TGS, (c) 2.755–3.050 Å in TGSe [20], (d) 2.863–2.896 Å in GPI, (e) 2.933–3.066 Å in GSN and (f) 2.838–3.016 Å in DGN, indicating the variation in the strength of N–H–O hydrogen bonds in these complexes. Though from the distances it appears that the hydrogen bonds in DGN are stronger than those in GSN due to dynamic rotation of the acceptor nitrate ion in DGN these bonds are actually weaker; this fact is supported by the higher NH as well as nitrate ion (ν_1) stretch frequencies of DGN (weaker hydrogen bonds result in increase in the stretch frequency) as compared to that in GSN. It is worth commenting that the ferroelectric transition temperature too varies in the same order i.e. 322 K for TGS, 295 K of TGSe, 224 K for GPI, 218 K for GSN and 206 K for DGN, as the hydrogen bonding strength in these glycine complexes indicates that the N–H–O bonds play a role directly or indirectly in the ferroelectric phase transitions in glycine complexes.

Another interesting point observed from Table 4 is that unlike the TGS and DGN crystals the $-CO_2^-$ modes (CO_2 wag, CO_2 bend, CO_2 sym str) of glycine zwitterions in GSN and alpha-glycine crystals have very negligible differences though in GSN–CO_2^- group is coordinated to Ag^+ ions and in alpha-glycine it makes strong N–H–O hydrogen bonds with the ionized amino group. This might be taken as an indication that the strength of the Ag–O coordination bond in GSN and N–H–O hydrogen bonds in alpha-glycine are comparable

though considering the differences between the two types of interactions i.e. hydrogen bonding and metal coordination, the similarity is surprising. The closeness between the CH_2 stretch frequencies in alpha-glycine and GSN indicates that there exist in GSN C–H–O bonds of similar strengths as those in alpha-glycine [21].

The fact that nitrate ion symmetry has been reduced from D_{3h} in the free ion state to C_s in the crystalline environment of GSN is reflected in the splitting of the two degenerate modes ν_4 (in-plane bending) and ν_3 (asymmetric stretching) (Table 4) of the ion in the Raman spectra [22]. Presence of forbidden out-of-plane deformation mode (ν_2) of NO_3^- ion in Raman spectra of GSN further supports the fact that molecular symmetry of the nitrate ion is lowered in the crystalline environment of GSN.

6. Discussion

The asymmetric unit in the low temperature ferro-phase of GSN has two independent molecules (Table 2) that become related to each other by an inversion center in the high temperature para-phase. Comparison between the room temperature and low temperature structure of GSN showed that the most significant structural change that leads to the lowering of the crystal symmetry at T_c is the movement of the Ag^+ ions away from the plane made by the oxygen atoms of the ionized carboxyl group of the glycine zwitterions coordinate to them as shown in Fig. 4 (torsion angle O2–Ag–Ags–O2s $=$ 162° for $T < T_c$ and $=$180° for $T > T_c$). Due to the above stated structural change the center of gravity of the negative charges (due to negatively charged carboxylic groups of glycines and nitrate ions) and the positive charges (due to positively charged amino groups of glycines and silver ions) within an asymmetric unit no longer coincide. Distance between the two estimated from the low temperature structure using the crystal structure-viewing program MERCURY is of the order of $d = 0.2$ Å. As a result a net electrical dipole moment ($\mu \approx qd$ where $q \approx 4e$) is induced within an asymmetric unit. A unit cell in ferro-phase has two such asymmetric units related to each other by 2-fold rotation along the b-axis, hence the component of dipole moment μ along the a and c axis are cancelled out leaving only the b-component of μ which add up to give the net unit cell dipole moment ($\mu_{\text{cell}} \approx 1.26$ D) along b-axis. The resultant value of spontaneous polarization (Ps) being 0.75×10^{-4} C/cm^2, this estimate of Ps from our phenomenological model agrees very well with the experimentally obtained value of Ps $= 0.55 \times 10^{-4}$ C/cm^2 at −195 °C [1] indicating the correctness of our phenomenological model. The net dipolar interaction energy [23] ($E_i = \sum_j [\mu_i \cdot \mu_j - 3(\mu_i \cdot r_{ij})(\mu_j \cdot r_{ij})/|r_{ij}|^2]/4\pi\varepsilon_0|r_{ij}|^3$) of a dipole μ_i located at the ith site of a hypothetical GSN crystal of size $8a \times 8b \times 8c$ was computed to be of the order of 2.01×10^{-21} J which agrees well with the thermal energy $k_B T_c = 3.00 \times 10^{-21}$ J at the transition point indicating the dipolar interactions bring about the phase transition at T_c. The direction of spontaneous polarization is reversed when the above stated displacement of the Ag^+ ions is reversed.

7. Conclusion

It is concluded from the X-ray as well as the DSC measurements that the phase transition in GSN is displacive in nature and results due to the displacement of the Ag^+ ions from the plane made by the carboxyl oxygens of glycines coordinated to it. A phenomenological model for the origin of ferroelectricity at T_c is given based on the fact that due to the movement of Ag^+ ion the center of gravity of negative and positive charges within an asymmetric unit of GSN no longer coincide in the low temperature phase, resulting in a net spontaneous dipole moment. By comparing the Raman spectra of ferroelectric glycine complexes it is concluded that the ferroelectric transition temperature varies in the same order as the strength of N–H–O hydrogen bonds in these crystals, indicating that these hydrogen bonds play a role in the ferroelectric phase transition in glycine complexes.

References

[1] F. Jona, G. Shirane, Ferroelectric Crystals, Pergamon Press, Oxford London, 1962 (Chapter 2).
[2] R. Pepinsky, K. Vedam, S. Hoshino, Y. Okaya, Phys. Rev. 111 (1958) 430–432.
[3] R. Pepinsky, Y. Okaya, D.P. Eastman, T. Mitsui, Phys. Rev. 107 (1957) 1538–1539.
[4] S. Launer, M. Le Maire, G. Schaack, S. Haussuhl, Ferroelectrics 132 (1992) 257.
[5] Ota Bludsky, Jana Chocholousova, Jaroslav Vacek, Friedrich Huisken, Pavel Hobza, J. Chem. Phys. 113 (2000) 4629–4635.
[6] P.W. Anderson, Science 177 (1972) 393–396.
[7] J.K.M. Rao, M.A. Viswamitra, Acta Cryst. B 28 (1972) 1481–1495.
[8] A.V.R. Warrier, P.S. Narayanan, Proc. Ind. Acad. Sci. 66A (1967) 46–54.
[9] K.R.K. Easwaran, J. Phys. Soc. Japn 21 (1966) 1614.
[10] Y. Onodera, N. Kojya, J. Phys. Soc. Jpn 58 (1989) 3227–3235.
[11] L.B. Mccusker, R.B. Von Dreele, D.E. Cox, D. Louer, P. Scardi, J. Appl. Cryst. 32 (1998) 36–50.
[12] A. Jouanneaux, CPD Newslett. 21 (1999) 13.
[13] S. Hoshino, T. Mitsui, F. Jona, R. Pepinsky, Phys. Rev. 107 (1957) 1255–1258.
[14] R. Pepinsky, K. Vedam, S. Hoshino, Y. Okaya, Phys. Rev. 111 (1958) 430.
[15] Herve Cailleau, Jean-Louis Baudour, Jean Meinnel, Ary Dworkin, Fernande Moussa, Claude M.E. Zeyen, Faraday Discussions Chem. Soc. 69 (1980) 7–18.
[16] Hans Stenback, J. Raman Spectrosc. 5 (1976) 49–55.
[17] Z.X. Shen, W.F. Sherman, M.H. Kuok, S.H. Tang, J. Raman Spectrosc. 23 (1992) 509–514.
[18] M. Gajdos, A. Eicher, J. Hafner, Surf. Sci. 531 (2003) 272–286.
[19] F.H. Allen, Acta Cryst. B 58 (2002) 380–388.
[20] R.R. Choudhury, R. Chitra, Lata Panicker (in press).
[21] Z. Berkovitch-Yellin, L. Leiserowitz, Acta Cryst. B 40 (1984) 159–165.
[22] Mark R. Waterland, Anne Myers Kelley, J. Chem. Phys. 113 (2000) 6760–6773.
[23] R.R. Choudhury, R. Chitra, M. Ramanadham, Physica B 366 (2005) 116–121.